



Synthesis and characterization of glycidyl-polymer-based poly(ionic liquid)s: Highly designable polyelectrolytes with poly(ethylene glycol) main chain

Journal:	<i>RSC Advances</i>
Manuscript ID	RA-ART-08-2015-017609.R1
Article Type:	Paper
Date Submitted by the Author:	06-Oct-2015
Complete List of Authors:	Ikeda, Taichi; National Institute for Materials Science, Nagao, Ikuhiro; National Institute for Materials Science, Moriyama, Satoshi; National Institute for Materials Science, Kim, Je-Deok; National Institute for Materials Science (NIMS), Fuel Cell Materials Center
Subject area & keyword:	Polymers < Materials

Synthesis and characterization of glycidyl-polymer-based poly(ionic liquid)s: Highly designable polyelectrolytes with poly(ethylene glycol) main chain

Received 00th January 20xx,
Accepted 00th January 20xx

DOI: 10.1039/x0xx00000x

www.rsc.org/

T. Ikeda,^{a*} I. Nagao,^a S. Moriyama^b and J.-D. Kim^c

A series of glycidyl-polymer-based poly(ionic liquid)s (cationic GTPs) was synthesized via the click functionalization of glycidyl azide polymer with alkyne derivatives of ionic liquids. Three types of ionic liquid moieties (imidazolium, pyridinium and pyrrolidinium) and two types of spacers between 1,2,3-triazole and cationic moiety (C₄H₈ alkyl chain (C4) and tetra(ethylene glycol) (EG4)) were examined. The cationic GTPs were characterized by NMR, IR, differential scanning calorimetry, thermogravimetric analysis and impedance spectroscopy. From the gel permeation chromatography analysis of the model polymer, the weight-average molecular weights of cationic GTPs were estimated to be 0.8–1.0 million Da. ¹H NMR analysis of the partially decomposed polymer confirmed that the thermal decomposition of the cationic GTPs with the C4 spacer begins with the detachment of the cationic moiety. Compared with the C4 spacer, the EG4 spacer decreases the glass transition temperature and increases the ionic conductivity. The cationic GTPs with the EG4 spacer, pyrrolidinium cationic moiety and bis(trifluoromethanesulfonyl)imide (Tf₂N) counter anion exhibited the highest anhydrous ionic conductivity (1.1 × 10⁻⁵ S cm⁻¹ at 30°C and 1.1 × 10⁻³ S cm⁻¹ at 120°C). The conducting ion concentration and mobility were estimated by electrode polarization analysis. The imidazolium moiety gives a relatively higher conducting ion concentration because of the lower binding energy with the Tf₂N counter anion. Compared with other GTPs, the pyridinium GTPs showed greater temperature dependences of their conducting ion mobilities.

1 Introduction

Polymer electrolytes are key materials in the field of electronic applications (*e.g.*, fuel cells,^{1,2} batteries,³ optoelectronic devices,⁴ actuators⁵ and electrochromic devices⁶). Poly(ionic liquid)s, which are defined as polymers with ionic liquid moieties as side groups, are an emerging class of polymer electrolytes developed in the last 15 years.^{7,8,9} To date, various types of poly(ionic liquid)s with different polymer backbones (*e.g.*, vinyl,^{10,11} styrene,^{12,13} (meth)acrylate^{12,14–18} and vinyl ether¹⁹) have been reported.

Poly(ethylene glycol) (PEG) is one of the most important polymer materials for solid electrolytes^{20–22} because of its (1) suitable thermal and electrochemical stabilities; (2) high affinity to ionic species, which leads to a high ionic concentration capacity and (3) high segmental motion of polymer chains, which leads to a high mobility of ionic species. In addition, oligo(ethylene glycol) is an important component of poly(ionic liquid)s for improving the ionic conductivity.^{16,18,23} However, poly(ionic liquid)s with PEG

main chains have not yet been well developed. Ohno *et al.* reported some PEG-based polyelectrolytes in which the ionic moieties were introduced in the main chain (ionomer type).²³ Recently, Drockenmuller *et al.* also prepared the ionomer type PEG-based polyelectrolytes using Cu(I)-catalysed azide-alkyne cycloaddition (Cu-AAC) reaction followed by the quaternization of the 1,2,3-triazole ring.²⁴ Endo *et al.* reported the PEG-based polyelectrolyte network (not linear polymer) from the copolymerization of the mono-epoxy-substituted ionic liquid and di-epoxy-substituted PEG.^{25,26} Some groups prepared the polyelectrolytes with PEG main chain by the reaction

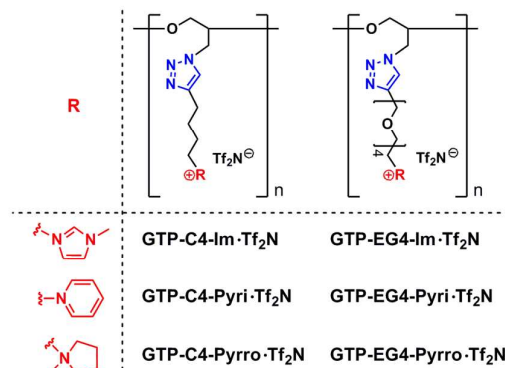


Fig. 1 Chemical structures of glycidyl-polymer-based poly(ionic liquid)s and their names.

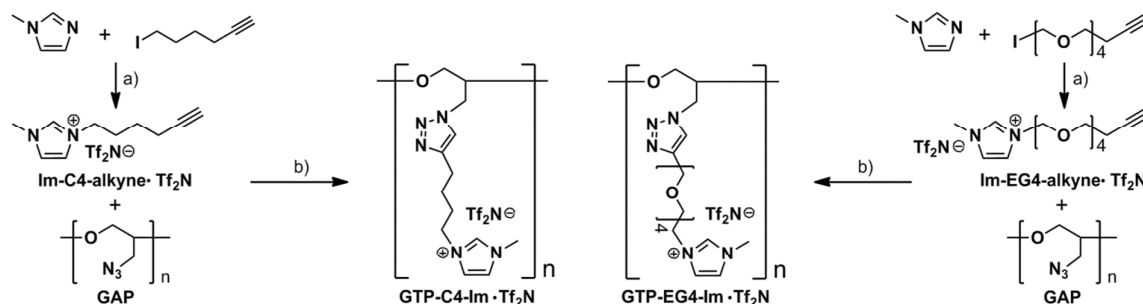
^a Polymer Materials Unit, National Institute for Materials Science (NIMS), 1-1

Namiki, Tsukuba, 305-0044, Japan. E-mail: IKEDA.Taichi@nims.go.jp

^b International Center for Materials Nanoarchitectonics (MANA), NIMS.

^c Polymer Electrolyte Fuel Cell Group, GREEN, NIMS.

[†]Electronic Supplementary Information (ESI) available: NMR, and DSC of all products, IR of all polymers, GPC of model polymer, ¹H NMR of partially-decomposed polymer, a part of impedance data. See DOI: 10.1039/x0xx00000x



Scheme 1 Synthesis of glycidyl-polymer-based poly(ionic liquids) **GTP-C4-Im-Tf₂N** and **GTP-EG4-Im-Tf₂N**. a) MeCN, 70°C, 3 days then Li-Tf₂N, H₂O; b) Cu(MeCN)₄PF₆, DMF, 50°C, 24 h then EDTA·2Na, Li-Tf₂N, H₂O.

between polyepichlorohydrin (PECH) and tertiary amines.^{27,28} Although quantitative S_N2 nucleophilic substitution of chlorine group requires harsh reaction conditions, Baker *et al.* succeeded to prepare the imidazolium-salt-grafted PEG from PECH.²⁹ Baker's synthetic scheme lacks the designability of the spacer between the polymer backbone and the ionic moiety. The molecular design of the spacer is important for improving the ionic conductivity.^{7,8} Thus, we aimed to develop the synthetic scheme of the PEG-based poly(ionic liquids) in which not only the ionic moiety but also the spacer unit are designable. PEG derivatives with functional side groups have been synthesized as glycidyl polymers via the anionic ring-opening polymerization of the epoxy monomer.³⁰ The synthesis of glycidyl polymers requires special equipment and skills to exclude impurities and water, which terminate the polymerization reaction. In general, ionic liquids are hygroscopic and difficult to purify by distillation. Presumably, these factors make it difficult to prepare glycidyl-polymer-based poly(ionic liquids). In practice, Endo *et al.* reported a difficulty for preparing pure epoxy monomer and the instability of the epoxy ring due to the presence of free counter ion.²⁶ Therefore, the development of facile synthetic route to highly designable glycidyl-polymer-based poly(ionic liquids) is a challenging theme.

Recently, we reported the facile and efficient synthesis of glycidyl 4-functionalized-1,2,3-triazole polymers (functionalized GTP) based on the post functionalization of glycidyl azide polymer (GAP) with various alkyne precursors via Cu-AAC reaction.³¹ GAP is easily accessible from commercially available PECH.³² Therefore, this approach enables us to obtain high-molecular-weight PEG derivatives with various functional side groups.

In this study, we have prepared six kinds of GTP-based poly(ionic liquids) (cationic GTPs) from the combination of three representative cationic moieties of ionic liquids (imidazolium, pyridinium and pyrrolidinium) and two types of spacers between 1,2,3-triazole and cationic moiety [C₄H₈ alkyl chain (C4) and tetra(ethylene glycol) (EG4)] (Fig. 1). We selected bis(trifluoromethanesulfonyl)imide (Tf₂N⁻) as a counter anion because it is more thermally stable and gives higher ionic conductivities than other counter anions (halogen ions, PF₆⁻ and BF₄⁻).^{8,18} Since these cationic GTPs were prepared from the same GAP sample via post functionalization,

the degrees of polymerization of these polymers are identical. Therefore, we can discuss the structure/properties relationships in detail.

2 Experimental section

2.1 Materials

PECH (weight-average molecular weight $M_w = 700$ kDa) and 1-methyl imidazole were purchased from Sigma-Aldrich Co. Tetrakis(acetonitrile) copper(I) hexafluorophosphate (Cu(MeCN)₄PF₆), pyridine, 1-methylpyrrolidine, tetra(ethylene glycol) and lithium bis(trifluoromethanesulfonyl) imide (Li-Tf₂N) were purchased from Tokyo Chemical Industry Co., Ltd. Ethylenediaminetetraacetic acid disodium salt dihydrate (EDTA·2Na) was purchased from Wako Pure Chemical Industries, Ltd. Other chemicals including dry solvents were purchased from commercial sources. 6-Iodo-1-hexyne,³³ α -iodo- ω -propargyl-tetraethylene glycol,³⁴ GAP and the model polymer of glycidyl 4-benzyl-1,2,3-triazole polymer (**GTP-C-Ph**) were synthesized according to the literature.³¹

2.2 Characterization methods

Nuclear magnetic resonance (NMR) spectra were recorded on a JEOL ECS-400 (400 MHz and 100 MHz for ¹H and ¹³C nuclei, respectively) with residual solvent as the internal standard. Fourier-transform infrared (FT-IR) spectra were obtained using a Shimadzu FTIR-8400S with a KBr sample pellet. Gel permeation chromatography (GPC) was carried out at 60°C with *N,N*-dimethylformamide (DMF) as the eluent on a Tosoh HLC-8220GPC with a Shodex GPC LF-804 column. Differential scanning calorimetry (DSC) was performed on a SII NanoTechnology EXSTAR X-DSC7000 from -120 to 120°C at a heating/cooling rate of 10°C min⁻¹ under N₂ flow. Thermogravimetric analysis (TGA) was performed on a TA Instruments SDT Q600 from 30 to 550°C at a heating rate of 10°C min⁻¹ under Ar flow. Ionic conductivity was measured using two-terminal impedance spectroscopy on a Solartron SI 1260 with a 1296 Dielectric Interface. The sample (*ca.* 10 mg) was placed on a disk-type gold-blocking electrode of a Solartron 12962A dielectric sample holder. The spacing between two electrodes was set to 300 μ m. The contact area of the sample to the electrode was calculated assuming a sample density of 1.4 g cm⁻³. The frequency was swept from 1 MHz to

1 Hz by applying a sinusoidal voltage of 100 mV. The sample holder was placed inside a programmable thermostat chamber ESPEC SH-221 filled with dry N₂ gas. The sample was completely dried at 120 °C for 1.5 h before starting the measurement. The impedance data were collected from 120 to 0 °C at a cooling rate of 20 °C h⁻¹ (0.33 °C min⁻¹). The data were processed using ZView[®] Ver. 3.3c software.

2.3 Synthesis of cationic alkynes

Im-C4-alkyne-Tf₂N: 1-Methyl imidazole (1.20 mL, 15 mmol), 6-iodo-1-hexyne (5.2 g, 25 mmol) were dissolved in dry MeCN (10 mL). The reaction mixture was stirred for 3 days at 70 °C under N₂ atmosphere. After cooling to room temperature, the distilled water (150 mL) was added to the reaction mixture and washed with CH₂Cl₂ five times. Li-Tf₂N solution (20.0 g/20 mL distilled water) was added to the sample solution with a pipette. The solution was stirred for 1h at room temperature. The product was extracted with CH₂Cl₂. The solution was dried with MgSO₄, filtered and concentrated by evaporation. The solvent was completely removed under vacuum. Yield: 6.7 g (quantitative). ¹H NMR (400 MHz, DMSO-*d*₆): δ = 1.42 (q, *J* = 7.2 Hz, 2H), 1.87 (q, *J* = 8.0 Hz, 2H), 2.21 (dt, *J* = 2.4 Hz, 7.6 Hz, 2H), 2.79 (t, *J* = 2.8 Hz, 1H), 3.84 (s, 3H), 4.18 (t, *J* = 7.2 Hz, 2H), 7.69 (t, *J* = 2.0 Hz, 1H), 7.75 (t, *J* = 2.0 Hz, 1H), 9.10 (s, 1H); ¹³C NMR (100 MHz, DMSO-*d*₆): δ = 17.1, 24.5, 28.6, 35.7, 48.3, 71.6, 83.8, 119.5 (q, *J* = 320.3 Hz), 122.2, 123.7, 136.6; *T*_g = -80.5 °C.

Pyri-C4-alkyne-Tf₂N: The synthetic procedure was the same as above. Yield: 6.6 g (quantitative). ¹H NMR (400 MHz, DMSO-*d*₆): δ = 1.45 (q, *J* = 7.6 Hz, 2H), 2.00 (q, *J* = 7.6 Hz, 2H), 2.22 (dt, *J* = 2.8 Hz, 7.6 Hz, 2H), 2.81 (t, *J* = 2.8 Hz, 1H), 4.62 (t, *J* = 7.2 Hz, 2H), 8.17 (t, *J* = 6.8 Hz, 2H), 8.61 (t, *J* = 7.6 Hz, 1H), 9.08 (d, *J* = 6.8 Hz, 2H); ¹³C NMR (100 MHz, DMSO-*d*₆): δ = 17.2, 24.4, 29.9, 60.3, 71.8, 83.8, 119.5 (t, *J* = 320.4), 128.2, 144.7, 145.5; *T*_g = -74.7 °C.

Pyrrro-C4-alkyne-Tf₂N: The synthetic procedure was the same as above. Yield: 4.5 g (90%). ¹H NMR (400 MHz, DMSO-*d*₆): δ = 1.48 (q, *J* = 7.2 Hz, 2H), 1.78 (m, 2H), 2.08 (br, 4H), 2.24 (dt, *J* = 2.8 Hz, 6.8 Hz, 2H), 2.84 (t, *J* = 2.8 Hz, 1H), 2.97 (s, 3H), 3.3 (overlapping with solvent peak), 3.36–3.52 (m, 4H); ¹³C NMR (100 MHz, DMSO-*d*₆): δ = 17.2, 21.1, 22.2, 25.0, 47.5, 62.5, 63.5, 71.8, 119.5 (t, *J* = 320.4); *T*_g = -81.8 °C.

Im-EG4-alkyne-Tf₂N: 1-Methyl imidazole (0.80 mL, 10 mmol) and α-iodo-ω-propargyl-tetraethylene glycol (4.0 g, 10 mmol) were dissolved in dry MeCN (10 mL). The reaction mixture was stirred for 3 days at 70 °C under N₂ atmosphere. After cooling to room temperature, the reaction mixture was added dropwise to diethyl ether (150 mL) with stirring. After 1h, the solvent was removed by decantation. The product was dissolved in distilled water (150 mL), then Li-Tf₂N solution (15 g/15 mL distilled water) was added with a pipette. The solution was stirred for 1h at room temperature. The product was extracted with CH₂Cl₂. The solution was dried with MgSO₄, filtered and concentrated by evaporation. The solvent was

completely removed under vacuum. Yield: 5.7 g (quantitative). ¹H NMR (400 MHz, DMSO-*d*₆): δ = 3.42 (t, *J* = 2.4 Hz, 1H), 3.46–3.57 (m, 12H), 3.77 (t, *J* = 5.6 Hz, 2H), 3.86 (s, 3H), 4.12 (d, *J* = 2.8 Hz, 2H), 4.34 (t, *J* = 5.2 Hz, 2H), 7.68 (t, *J* = 2.0 Hz, 1H), 7.72 (t, *J* = 1.6 Hz, 1H), 9.04 (s, 1H); ¹³C NMR (100 MHz, DMSO-*d*₆): δ = 35.7, 48.8, 57.5, 68.1, 68.5, 69.5, 69.5, 69.6, 69.7, 69.7, 77.1, 80.3, 119.5 (q, *J* = 320.3), 122.7, 123.3, 136.8; *T*_g = -68.6 °C.

Pyri-EG4-alkyne-Tf₂N: The synthetic procedure was the same as above. Yield: 5.6 g (quantitative). ¹H NMR (400 MHz, DMSO-*d*₆): δ = 3.38–3.57 (m, 13H), 3.92 (t, *J* = 5.2 Hz, 2H), 4.13 (d, *J* = 2.4 Hz, 2H), 4.79 (t, *J* = 4.8 Hz, 2H), 8.16 (t, *J* = 7.6 Hz, 2H), 8.62 (t, *J* = 7.6 Hz, 1H), 9.02 (d, *J* = 5.6 Hz, 2H); ¹³C NMR (100 MHz, DMSO-*d*₆): δ = 57.5, 60.4, 68.5, 68.6, 69.5, 69.5, 69.7, 69.7, 69.7, 77.1, 80.3, 119.5 (q, *J* = 320.3), 127.7, 145.2, 145.7; *T*_g = -65.6 °C.

Pyrrro-EG4-alkyne-Tf₂N: The synthetic procedure was the same as above. Yield: 5.1 g (85%). ¹H NMR (400 MHz, DMSO-*d*₆): δ = 2.08 (br, 4H), 3.03 (s, 3H), 3.43 (t, *J* = 2.4 Hz, 1H), 3.45–3.61 (m, 18H), 3.85 (br, 2H), 4.14 (d, *J* = 2.8 Hz, 2H); ¹³C NMR (100 MHz, DMSO-*d*₆): δ = 20.9, 48.0, 57.5, 62.1, 64.2, 64.5, 68.6, 69.4, 69.5, 69.5, 69.7, 69.8, 77.1, 119.5 (q, *J* = 320.3); *T*_g = -75.5 °C.

2.4 Synthesis of cationic GTPs

GTP-C4-Im-Tf₂N: GAP (0.50 g, 5.0 mmol monomer unit) was dissolved completely in dry DMF (25 mL) with stirring at 50 °C. (*Caution:* Never heat up too much and never agitate by sonication.) After 10 min Ar bubbling of the solution, **Im-C4-alkyne-Tf₂N** (6.0 mmol) and the copper catalyst (Cu(MeCN)₄PF₆, 0.10 g, 0.27 mmol) were added to the solution. The mixture was stirred at 50 °C under Ar atmosphere for 24 h. After cooling to room temperature, the solution was added dropwise to diethyl ether (300mL) with stirring to precipitate the product. After 30 min, the solvent was removed by decantation. The product was dissolved in acetone (40 mL). The solution was added dropwise to 0.1 N EDTA-2Na aqueous solution (200 mL). The colour of EDTA solution turned blue because of Cu²⁺ ion entrapped by EDTA. After adding Li-Tf₂N (10 g), acetone was removed under reduced pressure with a rotary evaporator. The aqueous solution was removed by decantation. The procedure for removing Cu ion has done some times until EDTA solution became colourless. After rinsing the product with pure water, the product was dissolved in acetone (100 mL) and dried with MgSO₄, filtered and concentrated by evaporation to 10 mL. The Me₂CO solution was added dropwise to CH₂Cl₂ (200 mL) with stirring. The solution was stirred for 3h. The solvent was removed by decantation. The product was dissolved in acetone and concentrated by evaporation. The product was completely dried under vacuum. Yield: 2.8 g (82%). ¹H NMR (400 MHz, DMSO-*d*₆): δ = 1.53 (br, 2H), 1.79 (br, 2H), 2.59 (br, 2H), 3.20–3.60 (br, overlapping with water peak), 3.72 (br, 1H), 3.83 (s, 3H), 4.14 (br, 2H), 4.10–4.45 (br, 2H), 7.67 (br, 3H), 9.05 (br, 1H); ¹³C NMR (100 MHz, DMSO-*d*₆): δ = 24.2, 25.6, 29.0, 35.7, 48.5,

50.0, 67.9, 77.0, 119.4 (t, $J = 320.4$), 122.1, 122.9, 123.7, 136.4, 146.3.

GTP-C4-Pyri-Tf₂N: The synthetic procedure was the same as above. Yield: 2.6 g (76%). ¹H NMR (400 MHz, DMSO-*d*₆): $\delta = 1.55$ (br, 2H), 1.93 (br, 2H), 2.59 (br, 2H), 3.20–3.55 (overlapping with water peak), 3.70 (br, 1H), 4.10–4.45 (br, 2H), 4.59 (br, 2H), 7.71 (br, 1H), 8.13 (br, 2H), 8.59 (br, 1H), 9.03 (br, 2H); ¹³C NMR (100 MHz, DMSO-*d*₆): $\delta = 24.3$, 25.5, 30.3, 50.0, 60.5, 68.0, 77.0, 119.4 (t, $J = 320.4$), 122.8, 128.1, 144.6, 145.6, 146.1.

GTP-C4-Pyrro-Tf₂N: The synthetic procedure was the same as above. Yield: 2.6 g (75%). ¹H NMR (400 MHz, DMSO-*d*₆): $\delta = 1.57$ (br, 2H), 1.74 (br, 2H), 2.07 (br, 4H), 2.62 (br, 2H), 2.96 (s, 3H), 3.20–3.55 (overlapping with water peak), 3.35–3.50 (br, 4H), 3.70 (s, 1H), 4.10–4.45 (br, 2H), 7.74 (br, 1H); ¹³C NMR (100 MHz, DMSO-*d*₆): $\delta = 21.1$, 22.6, 24.4, 26.0, 47.5, 50.0, 62.7, 63.5, 68.0, 77.0, 119.4 (t, $J = 320.4$), 122.7, 146.3.

GTP-EG4-Im-Tf₂N: The synthetic procedure was the same as above. Yield: 2.5 g (90%). ¹H NMR (400 MHz, DMSO-*d*₆): $\delta = 3.25$ –3.55 (br, overlapping with water peak), 3.74 (br, 2H), 3.84 (s, 3H), 4.31 (br, 2H), 4.47 (br, 2H), 7.65 (s, 1H), 7.68 (s, 1H), 7.99 (br, 1H), 9.01 (s, 1H); ¹³C NMR (100 MHz, DMSO-*d*₆): $\delta = 35.7$, 48.7, 50.1, 63.3, 68.1, 69.0, 69.3–69.8, 77.1, 119.4 (t, $J = 320.4$), 122.6, 123.3, 124.9, 136.8, 143.8.

GTP-EG4-Pyri-Tf₂N: Yield: 2.3 g (85%). ¹H NMR (400 MHz, DMSO-*d*₆): $\delta = 3.25$ –3.55 (br, overlapping with water peak), 3.88 (br, 2H), 4.46 (br, 2H), 4.76 (br, 2H), 7.98 (br, 1H), 8.13 (br, 2H), 8.59 (br, 1H), 8.99 (br, 2H); ¹³C NMR (100 MHz, DMSO-*d*₆): $\delta = 50.0$, 60.4, 63.3, 68.0, 68.5, 68.9, 69.3–69.8, 77.1, 119.4 (t, $J = 320.4$), 124.9, 127.7, 143.8, 145.2, 145.7.

GTP-EG4-Pyrro-Tf₂N: Yield: 2.1 g (76%). ¹H NMR (400 MHz, DMSO-*d*₆): $\delta = 2.07$ (br, 4H), 3.02 (s, 3H), 3.25–3.60 (br, overlapping with water peak), 3.83 (br, 2H), 4.49 (br, 2H), 8.00 (br, 1H); ¹³C NMR (100 MHz, DMSO-*d*₆): $\delta = 20.9$, 48.0, 50.1, 62.1, 63.3, 64.3, 64.5, 68.9, 69.4–69.8, 77.1, 119.4 (t, $J = 320.4$), 124.9, 143.8.

3 Results and discussion

Table 1 Physical properties of cationic GTPs.

Cationic GTPs	M_n^a kg mol ⁻¹	M_w^b kg mol ⁻¹	T_g °C	ΔT_g^c °C	T_{d5}^d °C	σ_{bc} at 30°C S cm ⁻¹	σ_{bc} at 120°C S cm ⁻¹	E_a^e kJ mol ⁻¹	p_{∞}^f cm ⁻³
GTP-C4-Im-Tf ₂ N	411	803	-5.3	75.2	313	5.8×10^{-7}	3.9×10^{-4}	17.2	2.3×10^{20}
GTP-C4-Pyri-Tf ₂ N	408	798	2.9	77.6	260	5.0×10^{-7}	7.0×10^{-4}	19.2	2.0×10^{20}
GTP-C4-Pyrro-Tf ₂ N	413	807	13.8	95.6	283	1.9×10^{-7}	2.9×10^{-4}	19.0	1.6×10^{20}
GTP-EG4-Im-Tf ₂ N	512	1000	-29.5	39.1	339	4.8×10^{-6}	7.1×10^{-4}	18.4	6.0×10^{20}
GTP-EG4-Pyri-Tf ₂ N	510	997	-22.9	42.7	315	4.3×10^{-6}	9.8×10^{-4}	19.5	3.1×10^{20}
GTP-EG4-Pyrro-Tf ₂ N	514	1000	-25.6	49.9	330	1.1×10^{-5}	1.1×10^{-3}	19.5	4.9×10^{20}

^aCalculated from number-average degree of polymerization of GTP-C-Ph. ^bCalculated from weight-average degree of polymerization of GTP-C-Ph. ^cDifference in T_g s between cationic alkyne and its GTP derivatives. ^d5 wt% decomposition temperature. ^eActivation energy obtained from eqn (5). ^fConducting ion concentration at $T \rightarrow \infty$ in eqn (5).

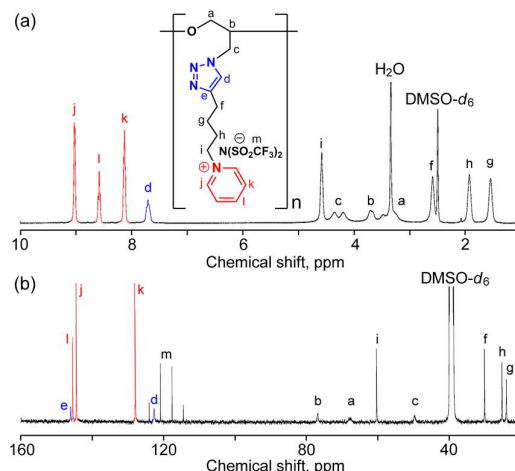


Fig. 2 (a) ¹H and (b) ¹³C NMR spectra of GTP-C₄-Py-Tf₂N (400MHz, DMSO-*d*₆).

3.1 Synthesis of cationic GTPs

Scheme 1 shows the synthetic routes for GTP-C4-Im-Tf₂N and GTP-EG4-Im-Tf₂N. First, 1-methyl imidazole was reacted with 6-iodo-1-hexyne or α -iodo- ω -propargyl-tetra(ethylene glycol) to synthesize cationic alkyne derivatives. After counter ion exchange with Tf₂N⁻, the cationic alkynes were obtained as a colourless liquid. The cationic alkynes were then reacted with GAP via a Cu-AAC reaction.³⁵ The other cationic GTPs were also synthesized using the same procedure. All these reactions were accomplished in high yield (75% – 100%).

The cationic GTPs reported herein were soluble in aprotic polar solvents such as acetone, MeCN, DMF and dimethyl sulfoxide (DMSO) and insoluble in protic solvents (water and MeOH) and nonpolar solvents such as hexane, toluene, diethyl ether, CHCl₃ and CH₂Cl₂.

The chemical structures of these polymers were confirmed by IR, ¹H and ¹³C NMR measurements. The IR spectra showed no azide peaks (2100 cm⁻¹) after the Cu-AAC reaction, which supports the quantitative functionalization of the side group (Fig. S1 in the ESI[†]). Fig. 2a shows the ¹H NMR spectrum of GTP-C4-Py-Tf₂N. All of the ¹H NMR peaks are broad due to the shorter relaxation time of the high-molecular-weight polymer. The signal at 7.71 ppm is assigned to the proton of the

triazole ring, and the set of the signals at 8.13, 8.59 and 9.04 ppm is assigned to the protons of the pyridinium ring. The peaks around 3.1–4.5 ppm correspond to the protons of the glycidyl main chain, while the set of the peaks at 1.55, 1.93, 2.59 and 4.59 ppm correspond to the methylene protons of the side chain. In the ^{13}C NMR spectrum (Fig. 2b), sharp and clear peaks were observed for all carbons except the glycidyl carbons. The signals at 122.8 and 146.1 ppm correspond to the triazole carbons, while the signals at 128.1, 144.5 and 145.5 ppm correspond to the pyridinium carbons. The peaks of the methylene carbons in the side chain are found at 24.2, 25.4, 30.3 and 60.5 ppm. The peak of the carbon of the Tf_2N^- counter anion is observed at 119.4 ppm and is split into a quartet due to spin coupling with the fluorine nucleus. As reported previously,³¹ we observed the broadening of the peaks of glycidyl carbons, which is attributable to the atactic property of the starting polymer PECH.³²

The molecular weight determination of poly(ionic liquid)s by GPC is often hindered by the adsorption of the cationic polymer on the column resin.²⁹ In the case of the polymer prepared by post-functionalization, the molecular weight can be determined using the precursor polymer.^{13,18,19} However, the molecular weight determination of GAP is difficult because its molecules associate with each other, preventing it from dissolving completely.³¹ Therefore, we synthesized a non-ionic model polymer and measured its molecular weight by GPC. We used **GTP-C-Ph** as a model polymer because **GTP-C-Ph** affords the most reliable GPC data among functional GTPs.³¹ The number- and weight-average molecular weights (M_n and M_w ,

respectively) of **GTP-C-Ph** were determined from the GPC chart (Fig. S13 in the ESI[†]) to be 163 kDa and 319 kDa, respectively (polystyrene standard, polydispersity index: $M_w/M_n = 2.0$). From these molecular weight data, the number- and weight-average degrees of polymerization (N_n and N_w , respectively) were calculated to be 757 and 1480, respectively. The calculated molecular weights of the cationic GTPs are summarized in Table 1.

3.2 Thermal property

The thermal properties of the cationic alkynes and GTPs were characterized by DSC and TGA. All cationic alkynes are liquid at room temperature; therefore, they are ionic liquids. In the case of **Pyri-C4-alkyne-Tf₂N**, peaks corresponding to the melting and crystallization transitions were observed, comparable to the thermal property of pyridinium ionic liquid with a C6 alkyl chain.³⁶ The other cationic alkynes showed no transition peaks at temperatures up to 120°C (Fig. S14 in the ESI[†]).

The cationic GTPs had higher glass transition temperatures (T_g) than the cationic alkynes. The differences in T_g s between the cationic alkyne and its GTP derivative (ΔT_g) are 75–95°C for GTP-C4 derivatives and 40–50°C for GTP-EG4 derivatives. It is clear that the T_g of the cationic GTP depends more significantly on the type of the spacer than that of the cationic moiety. GTP-EG4 derivatives have lower T_g values (about –25°C, Table 1) than GTP-C4 derivatives. Similarly, some groups have reported a lower T_g for ethylene glycol substitution compared to the alkyl chain.^{16,23,24} The high segmental motion of the ethylene glycol chains contributes to decreasing T_g . All of the cationic GTPs did not show crystallization or melting peaks at temperatures up to 120°C (Figure S15 in the ESI[†]).

The type of the spacer also affects the thermal stability (Fig. 3). The thermal stabilities of the GTP-EG4 derivatives were superior to those of the GTP-C4 derivatives. For the GTP-C4 derivatives, the decomposition seems to take place in a stepwise fashion. **GTP-C4-Pyri-Tf₂N** showed a particularly clear stepwise TGA curve. In the first step, 15% weight loss was observed at around 270°C, which corresponds to the weight fraction of the pyridinium moiety. In order to identify the decomposed part, we stopped the TGA analysis at 330°C and analysed the partially decomposed sample using ^1H NMR spectroscopy (Fig. S16 in the ESI[†]). The peaks of the pyridinium protons disappeared, while those of the other protons (*i.e.*, glycidyl main chain, triazole ring and C4 methylene protons) were detectable. This result indicates that the thermal decomposition of GTP-C4 derivatives begins with the detachment of the cationic moiety. In other words, glycidyl triazole unit has good thermal resistance over 300°C. The thermal stability of the cationic moiety increases in the following order: imidazolium > pyrrolidinium > pyridinium. For the GTP-EG4 derivatives, 5 wt% loss temperatures were over 300°C. The order of thermal stability is the same as that for the GTP-C4 derivatives.

3.3 Ionic conductivity

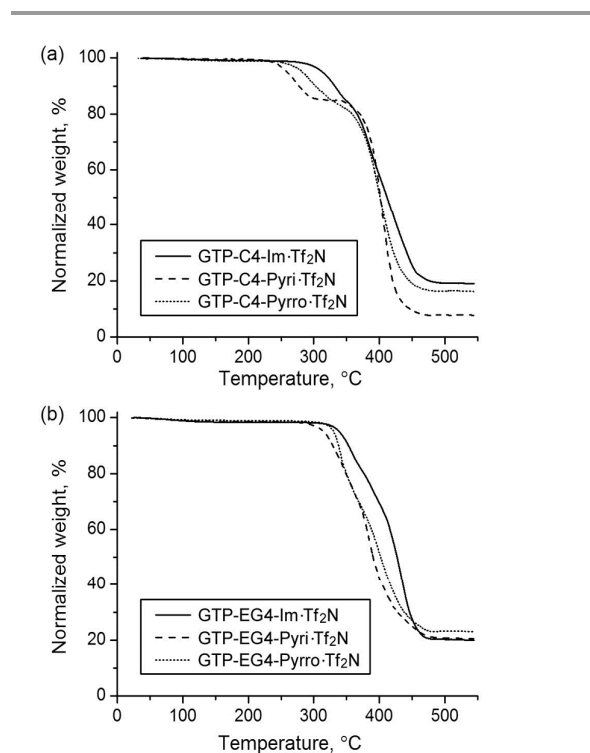


Fig. 3 TGA curves of (a) GTP-C4 derivatives and (b) GTP-EG4 derivatives.

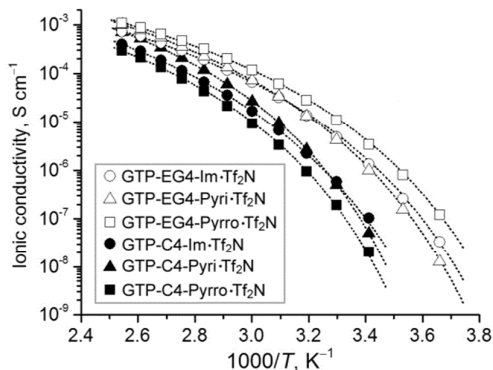


Fig. 4 Relationship between ionic conductivity and reciprocal temperature. The dotted curves were obtained by fitting using equation (1).

The ionic conductivities of the cationic GTPs were analysed by impedance spectroscopy under anhydrous condition.³⁷ The direct current conductivity (σ_{DC}) was obtained from the plateau region of the conductivity vs. frequency plot (Fig. S17 in the ESI[†]). Fig. 4 plots the relationship between the ionic conductivity and reciprocal temperature. The ionic conductivities of all polymers followed the Vogel-Fulcher-Tammann (VFT)-type temperature dependence, which reflects the coupling of the segmental motion of the polymer and ion transport.^{14,16–18,24} The data were fitted with the following equation:

$$\sigma_{DC} = \sigma_{\infty} \times \exp(-D_{\sigma}T_{\sigma}/(T-T_{\sigma})) \quad (1)$$

where σ_{∞} is the ionic conductivity at $T \rightarrow \infty$, D_{σ} is the strength parameter related to the divergence from the Arrhenius temperature dependence and T_{σ} is the Vogel temperature at which the free volume extrapolates to zero. The parameters obtained from fitting the data in Fig. 4 are summarized in Table S1 (see the ESI[†]). The ionic conductivities of the GTP-EG4 derivatives are higher than those of the GTP-C4 derivatives. This result is consistent with previous reports describing that oligo(ethylene glycol) functionalization improves the ionic conductivity.^{16,18,24} The higher segmental motion of the ethylene glycol chain compared to the alkyl chain facilitates ion transport. The relationship between the type of cationic moiety and ionic conductivity is difficult to understand. The pyrrolidinium GTP showed the best conductivity among the GTP-EG4 derivatives, while it showed the worst conductivity among the GTP-C4 derivatives. The pyridinium GTPs showed a more significant temperature dependence than the other GTPs. This result will be discussed later. The best ionic conductivity at 30°C in this report is 1.1×10^{-5} S cm⁻¹ for **GTP-EG4-Pyrro-Tf₂N**. This value is comparable to the best values in recent literatures (2.8×10^{-5} at 25°C,¹⁶ 1.0×10^{-5} at 25°C,⁶ and 1.1×10^{-5} at 30°C,¹⁸ 0.5 – 1.2×10^{-5} at 30°C²⁹). It should be noted that Ohno *et al.* reported a high ionic conductivity of 1.37×10^{-4} S cm⁻¹ for the acrylate-based poly(ionic liquid) with a 1-ethyl imidazolium moiety, C6 spacer

and Tf₂N⁻ counter anion.³⁸ The ionic conductivity of **GTP-EG4-Pyrro-Tf₂N** reached 1.1×10^{-3} S cm⁻¹ at 120°C.

The ionic conduction is the product of charge ($e = 1.60 \times 10^{-19}$ C), conducting ion concentration (p , cm⁻³) and conducting ion mobility (μ , cm²V⁻¹s⁻¹). In order to discuss the ionic conduction in more detail, we estimated the values of p and μ based on a physical model of electrode polarization.^{37,39,40} The Macdonald/Coelho model treats electrode polarization as a simple Debye relaxation with loss tangent ($\tan \delta$).^{39–41}

$$\tan \delta = \omega \tau_{EP} / (1 + \omega^2 \tau_{\sigma} \tau_{EP}) \quad (2)$$

where τ_{EP} and τ_{σ} are the electrode polarization time and the conductivity time, respectively, and ω is the angular frequency ($2\pi f$). From the fitting of the data with eqn (2), we obtained the values of τ_{EP} and τ_{σ} (Fig. S18 in the ESI[†]). The values of p and μ were then calculated from eqs (3) and (4), respectively:

$$p = (1/(\pi l_B L^2)) (\tau_{EP} / \tau_{\sigma})^2 \quad (3)$$

$$\mu = e L^2 \tau_{\sigma} / (4 \tau_{EP}^2 k T) \quad (4)$$

where l_B is the Bjerrum length given by $e^2/(4\pi\epsilon_0\epsilon_{DC}kT)$, L is the spacing between electrodes, e is the elementary charge, k is the Boltzmann constant and T is the absolute temperature.

Fig. 5a shows the temperature dependence of the conducting ion concentration calculated from eqn (3). The conducting ion concentrations of the cationic GTPs are on the order of 10^{17}

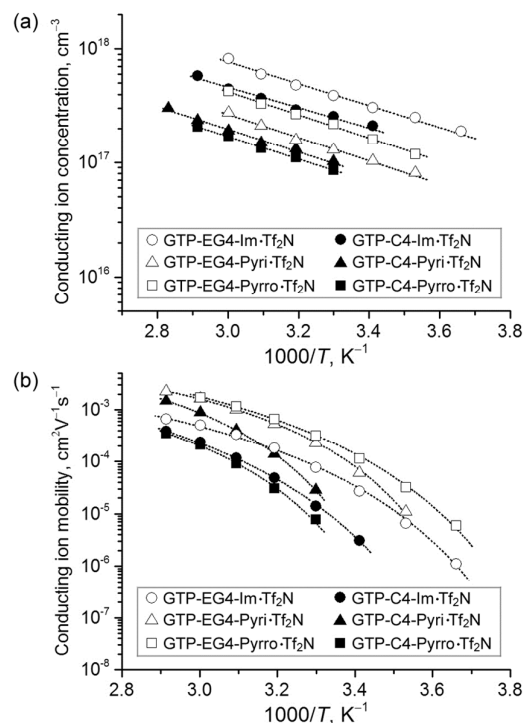


Fig. 5 (a) Temperature dependence of conducting ion concentration. The dotted lines were obtained from fitting with equation (5). (b) Temperature dependence of conducting ion mobility. The dotted curves were obtained from fitting with equation (6).

(cm^{-3}), while the bulk concentrations of the Tf_2N^- counter anions are on the order of 10^{21} (cm^{-3}) which was calculated assuming the cationic GTP density to be 1.4 g cm^{-3} . This result indicates that the fraction of ions contributing to ionic conduction would be about 0.1%, which is comparable to the values reported for single-ion conducting polyelectrolytes.^{16,41,42} Compared two GTPs with the same cationic moieties, the p values of the GTP-EG4 derivatives are higher than those of the GTP-C4 derivatives. Among three GTPs with the same spacer, the p value of GTP with the imidazolium moiety is higher than those with other cationic moieties. The temperature dependence of the conducting ion concentration can be analyzed by the Arrhenius plot:

$$p = p_\infty \times \exp(-E_a/RT) \quad (5)$$

where p_∞ is the conducting ion concentration at $T \rightarrow \infty$ and E_a is the activation energy of the conducting ions. The parameters obtained from the fitting of the data in Fig. 5a are summarized in Table 1. Ideally, the p_∞ value should be the same as the bulk concentration of the Tf_2N^- counter anions. However, the p_∞ value obtained from extrapolation of the Arrhenius plot (10^{20} cm^{-3}) is smaller than the bulk concentration (10^{21} cm^{-3}). A small difference in slope will lead to large deviation from the real value; thus, it is difficult to obtain a p_∞ value that is the same as the bulk counter ion concentration. Regarding the activation energy, the cationic GTPs with imidazolium moieties have smaller E_a values than the other cationic GTPs. A lower activation energy indicates a lower binding energy of the Tf_2N^- ions with the cationic moiety. The lower activation energy is attributed to the higher conducting ion concentrations of the cationic GTPs with the imidazolium moieties.

Fig. 5b shows the temperature dependence of the conducting ion mobility calculated from eqn (4). We fit the data with the VFT-type equation:

$$\mu = \mu_\infty \times \exp(-D_\mu T_\mu / (T - T_\mu)) \quad (6)$$

where μ_∞ is the conducting ion mobility at $T \rightarrow \infty$, D_μ is the strength parameter and T_μ is the Vogel temperature. The parameters obtained from fitting the data in Fig. 5b are summarized in Table S1 (see the ESI[†]). Comparing two GTPs with the same cationic moiety, the μ value of the GTP-EG4 derivative is higher than that of the GTP-C4 derivative. Among three GTPs with the same spacer, the temperature dependence of the pyridinium GTP is more significant than the others. This result indicates that large temperature dependence of the pyridinium GTP's ionic conductivity arises from large temperature dependence of the conducting ion mobility. Presumably, the pyridinium cation interacts with the ether oxygen atoms more strongly than the others.^{43,44} In particular, the α -hydrogen of the pyridinium ring can form hydrogen bonds with the ether oxygen atom.⁴⁵ Therefore, the segmental motion of the polymer is suppressed at low temperature by the formation of the hydrogen bond network, whereas the hydrogen bond network will be broken at higher temperatures.

Conclusions

We proved that glycidyl-polymer-based poly(ionic liquid)s with different spacers and ionic moieties were obtainable from glycidyl azide polymer and alkyne derivatives of ionic liquids. Thanks to the high reactivity of the Cu-AAC reaction, we achieved the quantitative conversion of the glycidyl polymer side groups under mild reaction condition. The ^1H NMR analysis of the partially-decomposed **GTP-C4-Pyri-Tf₂N** confirmed that the thermal decomposition of the GTP-C4 derivatives begins with the detachment of the cationic moieties. Compared to the alkyl chain spacer, the tetra(ethylene glycol) spacer decreases the glass transition temperature and increases the ionic conductivity. **GTP-EG4-Pyrro-Tf₂N** exhibited highest ionic conductivity ($1.1 \times 10^{-5} \text{ S cm}^{-1}$ at 30°C and $1.1 \times 10^{-3} \text{ S cm}^{-1}$ at 120°C). The conducting ion concentration and its mobility were estimated by electrode polarization analysis. Only a small fraction (about 0.1 %) of the total counter anion exists as conducting ions contributing to ionic conduction. The imidazolium GTPs have higher conducting ion concentrations due to the lower binding energy of Tf_2N^- ion with the cationic moiety. The pyridinium GTPs showed larger temperature dependences than the others, presumably due to the formation of a hydrogen-bonding network between the pyridinium moiety and the ether oxygen atoms, which collapses with increasing temperature. Click functionalization of the azide polymer will expand the diversity of feasible molecular design on poly(ionic liquid)s, which is important for improving the functionality of poly(ionic liquid)s.

Acknowledgements

We thank NIMS MANA Technical Support Team for DSC measurements. We thank Center of Materials Research for Low Carbon Emission in NIMS for TGA measurements. We thank NIMS Molecule & Material Synthesis Platform for NMR and GPC measurements. We thank Dr. Rakesh K. Pandey for the instruction of ionic conductivity measurements. We would like to thank Enago (www.enago.jp) for the English language review. This work was financially supported by Grant-in-Aid for Scientific Research C, 25410233 (JSPS).

Notes and references

- G. Couture, A. Alaeddine, F. Boschet and B. Ameduri, *Prog. Polym. Sci.*, 2011, **36**, 1521.
- J. D. Kim, L. J. Ghil, M. S. Jun, J. K. Choi, H. J. Chang, Y. C. Kim and H. W. Rhee, *J. Electrochem. Soc.*, 2014, **161**, F724.
- H. Zhang, L. P. Zheng, J. Nie, X. J. Huang and Z. B. Zhou, *Prog. Chem.*, 2014, **26**, 1005.
- A. Duarte, K. Y. Pu, B. Liu and G. C. Bazan, *Chem. Mater.*, 2011, **23**, 501.
- M. Shahinpoor and K. J. Kim, *Smart Mater. Struct.*, 2004, **13**, 1362.
- A. S. Shaplov, D. O. Ponkratov, P. H. Aubert, E. I. Lozinskaya, C. Plesse, A. Maziz, P. S. Vlasov, F. Vidal and Y. S. Vygodskii, *Polymer*, 2014, **55**, 3385.
- N. Nishimura and H. Ohno, *Polymer*, 2014, **55**, 3289.

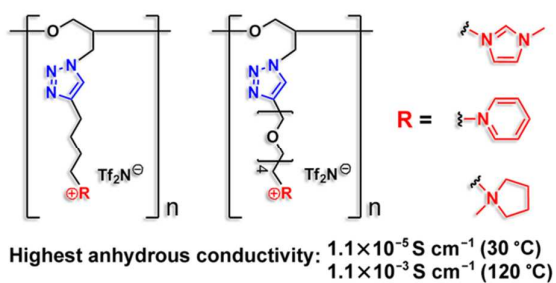
- 8 A. S. Shaplov, R. Marcilla and D. Mecerreyes, *Electrochim. Acta*, 2015, **175**, 18.
- 9 J. Y. Yuan and M. Antonietti, *Polymer*, 2011, **52**, 1469.
- 10 M. Hirao, K. Ito and H. Ohno, *Electrochim. Acta*, 2000, **45**, 1291.
- 11 R. Marcilla, J. A. Blazquez, J. Rodriguez, J. A. Pomposo and D. Mecerreyes, *J. Polym. Sci. A Polym. Chem.*, 2004, **42**, 208.
- 12 J. E. Bara, S. Lessmann, C. J. Gabriel, E. S. Hatakeyama, R. D. Noble and D. L. Gin, *Ind. Eng. Chem. Res.*, 2007, **46**, 5397.
- 13 H. D. Tang, J. B. Tang, S. J. Ding, M. Radosz and Y. Q. Shen, *J. Polym. Sci. A Polym. Chem.*, 2005, **43**, 1432.
- 14 W. Oghihara, S. Washiro, H. Nakajima and H. Ohno, *Electrochim. Acta*, 2006, **51**, 2614.
- 15 B. Yu, F. Zhou, C. W. Wang and W. M. Liu, *Eur. Polym. J.*, 2007, **43**, 2699.
- 16 M. Lee, U. H. Choi, R. H. Colby and H. W. Gibson, *Chem. Mater.*, 2010, **22**, 5814.
- 17 A. S. Shaplov, E. I. Lozinskaya, D. O. Ponkratov, I. A. Malyshkina, F. Vidal, P. H. Aubert, O. V. Okatova, G. M. Pavlov, L. I. Komarova, C. Wandrey and Y. S. Vygodskii, *Electrochim. Acta*, 2011, **57**, 74.
- 18 R. Sood, B. Zhang, A. Serghei, J. Bernard and E. Drockenmuller, *Polym. Chem.*, 2015, **6**, 3521.
- 19 K. I. Seno, S. Kanaoka and S. Aoshima, *J. Polym. Sci. A Polym. Chem.*, 2008, **46**, 5724.
- 20 D. E. Fenton, J. M. Parker and P. V. Wright, *Polymer*, 1973, **14**, 589.
- 21 K. Karuppasamy, R. Antony, S. Alwin, S. Balakumar and S. X. Sahaya, *Mater. Sci. Forum*, 2015, **807**, 41.
- 22 E. Quartarone, P. Mustarelli and A. Magistris, *Solid State Ionics*, 1998, **110**, 1.
- 23 H. Ohno, *Bull. Chem. Soc. Jpn.*, 2006, **79**, 1665.
- 24 B. P. Mudraboyina, M. M. Obadia, I. Allaoua, R. Sood, A. Serghei and E. Drockenmuller, *Chem. Mater.*, 2014, **26**, 1720.
- 25 K. Matsumoto and T. Endo, *Macromolecules*, 2009, **42**, 4580.
- 26 K. Matsumoto and T. Endo, *J. Polym. Sci. A Polym. Chem.*, 2011, **49**, 1874.
- 27 E. Agel, J. Bouet and J. F. Fauvarque, *J. Power Sources*, 2001, **101**, 267.
- 28 J. Hu, D. L. Wan, W. G. Zhu, L. H. Huang, S. Z. Tan, X. Cai and X. J. Zhang, *ACS Appl. Mater. Inter.*, 2014, **6**, 4720.
- 29 H. Y. Hu, W. Yuan, L. S. Lu, H. Zhao, Z. Jia and G. L. Baker, *J. Polym. Sci. A Polym. Chem.*, 2014, **52**, 2104.
- 30 H. Keul and M. Moller, *J. Polym. Sci. A Polym. Chem.*, 2009, **47**, 3209.
- 31 D. A. Liu, Y. J. Zheng, W. Steffen, M. Wagner, H. J. Butt and T. Ikeda, *Macromol. Chem. Phys.*, 2013, **214**, 56.
- 32 S. Brochu and G. Ampleman, *Macromolecules*, 1996, **29**, 5539.
- 33 T. Harada, K. Muramatsu, K. Mizunashi, C. Kitano, D. Imaoka, T. Fujiwara and H. Kataoka, *J. Org. Chem.*, 2008, **73**, 249.
- 34 L. N. Goswami, Z. H. Houston, S. J. Sarma, S. S. Jalisatgi and M. F. Hawthorne, *Org. Biomol. Chem.*, 2013, **11**, 1116.
- 35 V. V. Rostovtsev, L. G. Green, V. V. Fokin and K. B. Sharpless, *Angew. Chem. Int. Ed.*, 2002, **41**, 2596.
- 36 A. R. Choudhury, N. Winterton, A. Steiner, A. I. Cooper and K. A. Johnson, *J. Am. Chem. Soc.*, 2005, **127**, 16792.
- 37 E. Barsoukov and J. R. Macdonald, *Impedance Spectroscopy Theory, Experiment, and Applications*, 2nd ed., Wiley, Hoboken, 2005.
- 38 S. Washiro, M. Yoshizawa, H. Nakajima and H. Ohno, *Polymer*, 2004, **45**, 1577.
- 39 J. R. Macdonald, *Phys. Rev.*, 1953, **92**, 4.
- 40 R. Coelho, *Rev. Phys. Appl.*, 1983, **18**, 137.
- 41 R. J. Klein, S. H. Zhang, S. Dou, B. H. Jones, R. H. Colby and J. Runt, *J. Chem. Phys.*, 2006, **124**.
- 42 D. Fragiadakis, S. Dou, R. H. Colby and J. Runt, *J. Chem. Phys.*, 2009, **130**.
- 43 M. J. Lee, Z. B. Niu, D. V. Schoonover, C. Slebodnick and H. W. Gibson, *Tetrahedron*, 2010, **66**, 7077.
- 44 Y. Liu, C. J. Li, H. Y. Zhang, L. H. Wang and X. Y. Li, *Eur. J. Org. Chem.*, 2007, 4510.
- 45 S. J. Loeb and J. A. Wisner, *Angew. Chem. Int. Ed.*, 1998, **37**, 2838.

A table of contents entry:

Manuscript ID: RA-ART-08-2015-017609

Title: “*Synthesis and characterization of glycidyl-polymer-based poly(ionic liquid)s: Highly designable polyelectrolytes with poly(ethylene glycol) main chain*”

Taichi Ikeda*, Ikuhiro Nagao, Satoshi Moriyama, Jedeok Kim



Glycidyl-polymer-based poly(ionic liquid)s with different spacers and ionic moieties were synthesized by click functionalization of glycidyl azide polymer.